

# Exploring Reticular Pseudodrusen Extent and Impact on Mesopic Visual Sensitivity in Intermediate Age-Related Macular Degeneration

Himeesh Kumar,<sup>1,2</sup> Robyn H. Guymer,<sup>1,2</sup> Lauren A. B. Hodgson,<sup>1</sup> Xavier Hadoux,<sup>1,2</sup> and Zhichao Wu<sup>1,2</sup>

<sup>1</sup>Centre for Eye Research Australia, Royal Victorian Eye and Ear Hospital, East Melbourne, Australia

<sup>2</sup>Ophthalmology, Department of Surgery, The University of Melbourne, Melbourne, Australia

Correspondence: Zhichao Wu, Centre for Eye Research Australia, Level 7, 32 Gisborne Street, East Melbourne, VIC 3002, Australia; [wu.z@unimelb.edu.au](mailto:wu.z@unimelb.edu.au).

Received: January 20, 2022

Accepted: May 21, 2022

Published: June 15, 2022

Citation: Kumar H, Guymer RH, Hodgson LAB, Hadoux X, Wu Z. Exploring reticular pseudodrusen extent and impact on mesopic visual sensitivity in intermediate age-related macular degeneration. *Invest Ophthalmol Vis Sci.* 2022;63(6):14. <https://doi.org/10.1167/iovs.63.6.14>

**PURPOSE.** To explore the impact of the extent of reticular pseudodrusen (RPD) on mesopic visual sensitivity in individuals with intermediate age-related macular degeneration (AMD).

**METHODS.** In total, 570 eyes from 285 participants with bilateral large drusen underwent microperimetry testing to assess the visual sensitivity of the central 3.6-mm region and multimodal imaging to determine the extent of RPD in the central 20° × 20° region (at the eye level). Mean visual sensitivity within five sectors in the central 3.6-mm region sampled on microperimetry and the extent of RPD in these sectors were derived. Linear mixed models were used to examine the association between the extent of RPD on overall mean visual sensitivity and sector-based mean sensitivity.

**RESULTS.** An increasing extent of RPD at the eye level and within sectors was associated with a significant reduction in overall and sector-based mean sensitivity, respectively ( $P < 0.001$  for both). However, when both RPD parameters were considered together in a multivariable model, only an increasing extent of RPD at the eye level ( $P < 0.001$ ) and not within each sector ( $P = 0.178$ ) was independently associated with reduced sector-based mean sensitivity.

**CONCLUSIONS.** Mesopic visual sensitivity is generally reduced in eyes with large drusen and coexistent RPD compared to eyes without RPD, with greater reductions with an increasing extent of RPD. However, reduced sector-based visual sensitivities are explained by the overall extent of RPD present, rather than their extent within the sector itself. These findings suggest that there are generalized pathogenic changes in eyes with RPD accounting for the observed mesopic visual dysfunction.

Keywords: age-related macular degeneration, reticular pseudodrusen, visual sensitivity

The early stages of age-related macular degeneration (AMD) are characterized by the presence of drusen and pigmentary abnormalities within the macula. More recently, reticular pseudodrusen (RPD) has also become increasingly recognized as additional distinct deposits that are often present in eyes with AMD.<sup>1,2</sup> The implication of the presence of RPD, in AMD, is currently very topical as they appear to be a potentially critical phenotype in AMD, which has recently been discussed in detail.<sup>3</sup>

In brief, the presence of RPD is associated with an increased risk for progression to late AMD in the fellow, non-late AMD eyes of those with unilateral neovascular AMD.<sup>4-7</sup> The presence of RPD in non-late AMD eyes is also associated with a profound impairment in rod photoreceptor function.<sup>8-11</sup> There was also reported, strong evidence of treatment effect modification based on their presence in the Laser Intervention in the Early Stages of AMD (LEAD) study,<sup>12</sup> a trial of a subthreshold nanosecond laser aiming to slow progression of intermediate AMD. Together, these along with other findings all imply that there are likely important

pathogenic differences associated with eyes that develop RPD, underscoring the need to gain a more complete understanding of this phenotype, as we strive to reduce vision loss in AMD.

The distinct subretinal drusenoid deposits that characterize RPD<sup>13</sup> have been observed to disrupt or alter the contour of the overlying photoreceptor ellipsoid zone on optical coherence tomography (OCT) imaging.<sup>14,15</sup> Previous studies have also observed reduced photoreceptor density<sup>16</sup> and reflectivity<sup>17</sup> over these lesions on adaptive optics scanning laser ophthalmoscopy. Several studies have also observed a lower photoreceptor layer thickness and/or faster rate of photoreceptor layer thinning over time in eyes or areas with RPD.<sup>18-21</sup> Overall, these findings implicate photoreceptor changes in association with RPD.

While there is strong evidence for an association between the presence of RPD and impaired rod photoreceptor function, evident from measurements of visual sensitivity during dark adaptation,<sup>8-11</sup> studies on their association with abnormalities in cone-mediated function have

shown mixed results. The evidence for such an association can be considered from previous studies that have assessed visual sensitivity under both mesopic or photopic conditions using microperimetry (or fundus-controlled perimetry), recognizing that measurements under mesopic conditions primarily—although not entirely—assess cone-mediated function.<sup>22–25</sup> Such studies have demonstrated that visual sensitivities measured under mesopic or photopic conditions are reduced in eyes<sup>26–31</sup> or areas with RPD.<sup>32</sup> However, these studies have included small cohorts (30 to 51 eyes) and have not adjusted for key confounders of visual sensitivity, such as drusen volume.<sup>33–35</sup> In contrast, our previous work did not find significantly reduced mesopic visual sensitivities in individual regions with RPD (when analyzing five subfields within the central 3-mm region), with adjustment for confounders of visual function when evaluating 120 eyes with large drusen.<sup>34</sup> However, we did not examine whether there was a significant difference in visual sensitivity at the eye level based on the presence of RPD or whether visual sensitivity was associated with the spatial extent of RPD present (beyond their presence within the central subfields examined).

This current study thus aims to comprehensively examine the association between the presence and *en face* spatial extent of RPD with mesopic visual sensitivities in a substantially larger cohort of individuals with bilateral large drusen, both at the eye level and at regions tested on microperimetry. Adjustments for potential confounders will be performed in order to understand the independent impact of RPD on the predominantly cone-mediated photoreceptor function in the early stages of AMD.

## METHODS

This study examined a subset of participants enrolled in the LEAD study (clinicaltrials.gov identifier, NCT01790802) at their baseline visit,<sup>12</sup> and the LEAD study was conducted according to the International Conference on Harmonization Guidelines for Good Clinical Practice and the tenets of the Declaration of Helsinki. Participants were recruited from five sites within Australia and one site in Northern Ireland, and institutional review board approval was obtained at all sites. All participants enrolled in this study provided written informed consent. A list of investigators involved in the LEAD study is included in the Supplementary Material section.

### Participants and Procedures

A detailed description of the eligibility criteria for the LEAD study has been provided elsewhere.<sup>12,36</sup> In brief, all participants were required to be  $\geq 50$  years of age at the time of enrollment, have best-corrected visual acuity of  $\geq 20/40$  in both eyes, and bilateral large drusen ( $\geq 125 \mu\text{m}$ ) within a 1500- $\mu\text{m}$  radius of the fovea on color fundus photography (CFP), meeting the definition of intermediate AMD according to the Beckman classification.<sup>37</sup> In this study, participants with any signs of late AMD, as determined on multimodal imaging (MMI) of the retina, were excluded from the study. Late AMD on MMI was defined as the presence of (1) neovascular AMD, (2) geographic atrophy, or (3) OCT-defined nascent geographic atrophy (nGA; defined by the presence of subsidence of the outer plexiform layer and inner nuclear layer and/or a hyporeflective wedge-shaped band

within Henle's fiber layer).<sup>38,39</sup> Participants were further required to have one tested location showing reduced visual sensitivity ( $< 25$  dB) on microperimetry within the central  $6^\circ$  of the retina (described further below) on two tests. All participants in this study first underwent microperimetry testing, avoiding bleaching of the retina, followed by MMI.

### Microperimetry Testing

Measurements of mesopic visual sensitivities were obtained using the Macular Integrity Assessment (MAIA) device (CenterVue, Padova, Italy), following pupillary dilation. Goldmann Size III achromatic stimuli were presented against an achromatic mesopic background with a luminance of 1.27 candelas per square meter.<sup>40</sup> The central  $6^\circ$  radius of the macula was sampled using a customized stimulus pattern at 37 locations, as illustrated in the Figure, corresponding to a circular region with a diameter of 3.6 mm. Two tests were performed for each eye, and results from the second test were analyzed in the study (as we previously observed that the second test exhibits a lower degree of measurement variability<sup>41</sup>). A false-positive rate of  $\leq 25\%$  was required for a test to be deemed reliable, and in instances where the second test was not reliable and repeated testing was not performed, the first test was analyzed if it was reliable. The mean visual sensitivity of all the tested locations within the central 3.6-mm diameter region, as well as mean visual sensitivity in each of five sectors (each having the same area) within this region, was evaluated. The sectors were defined as follows: one sector in the central 1.6-mm diameter region and the other four sectors in the area between the central 1.6-mm and 3.6-mm diameter region, divided equally into quadrants (illustrated in the Fig.).

### Imaging Acquisition, Grading, and Analysis

MMI of the retina consisted of CFPs, OCT imaging, near-infrared reflectance (NIR), and fundus autofluorescence (FAF) imaging. Nonstereoscopic, macular-centered CFPs were obtained using a camera with a minimum resolution of  $2000 \times 2000$  pixels (camera specifications were site specific). OCT, NIR, and FAF imaging was performed using the Spectralis HRA+OCT (Heidelberg Engineering, Heidelberg, Germany) device. High-resolution OCT volume scans covered a  $20^\circ \times 20^\circ$  region centered on the fovea and consisted of 49 horizontal B-scans, with 25 frames averaged per B-scan. NIR and FAF images covered a  $30^\circ \times 30^\circ$  region of the macula, with a minimum resolution of  $768 \times 768$  pixels.

OCT volume scans were used to calculate drusen volume using a convolutional neural network-based approach as described previously.<sup>42</sup> In brief, segmentation of the RPE and Bruch's membrane was performed by a retinal layer segmentation algorithm, which enabled drusen volume from the entire central  $20^\circ \times 20^\circ$  region of the OCT volume scan to be calculated, as well as within each sector sampled on microperimetry (defined above) and outside the central 3.6-mm diameter region. The investigators who performed the OCT image analysis to calculate drusen volume are listed in the Supplementary Material. Drusen volume measurements were cube-root transformed to eliminate heteroskedasticity of the untransformed measurements.

CFPs were manually graded for the presence of pigmentary abnormalities. Each imaging modality was graded by

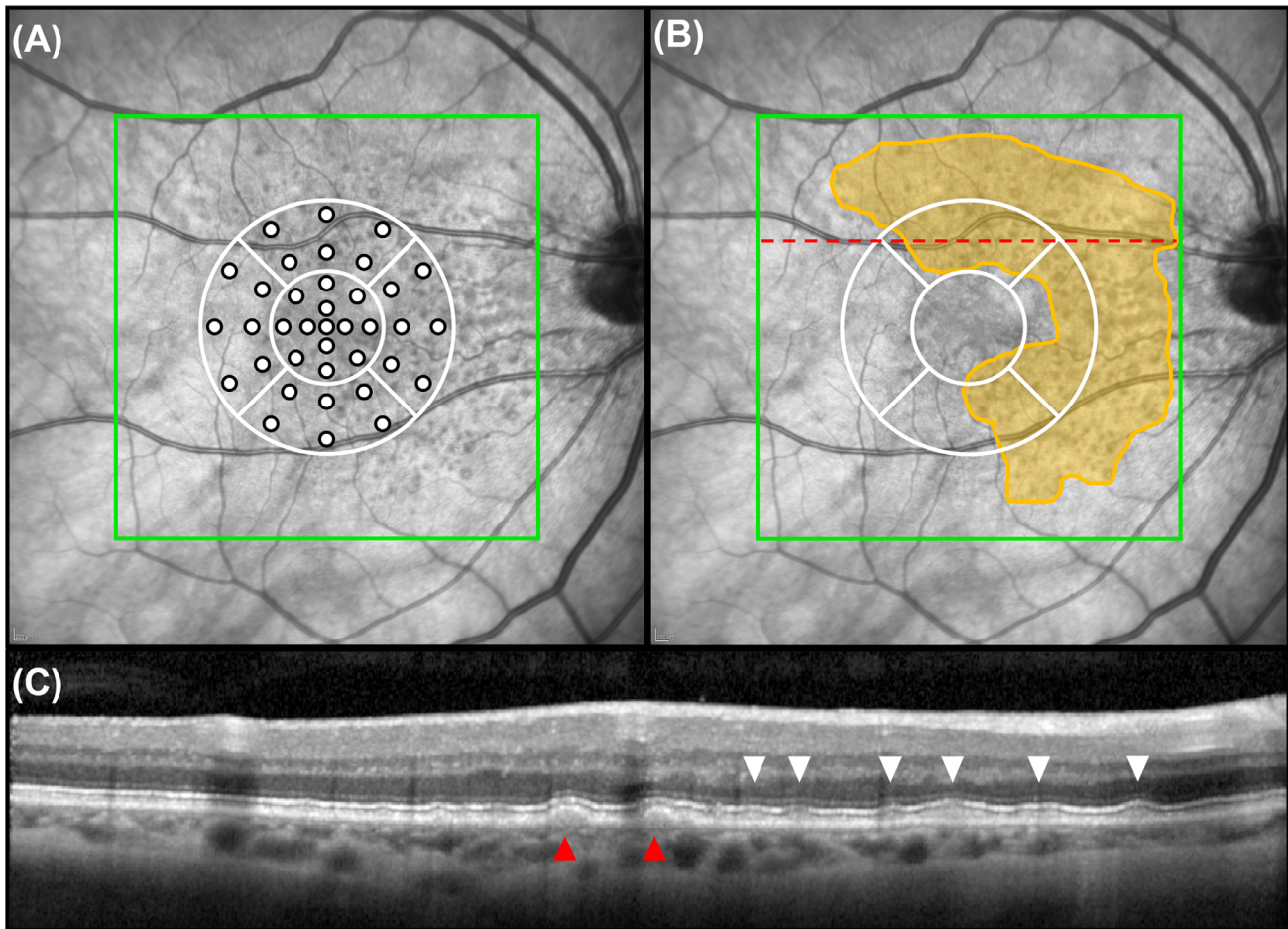


**FIGURE.** (A) Microperimetry testing stimulus pattern used to sample the central 3.6-mm diameter region of the macula divided into five sectors. (B) Extent of RPD seen on combined NIR and OCT imaging annotated (in yellow) on the NIR image. Red line indicates the level of the B-scan in C. (C) Example of RPD lesions seen on the OCT B-scan (location indicated by red line on the NIR image in B) with RPD lesions (white arrows) and drusen (red arrow).

a senior grader and senior medical retina specialist for the presence of RPD as being definitely present, questionable, or absent. These gradings were used to determine an MMI-defined presence of RPD, where OCT imaging and at least two *en face* imaging modalities (NIR, FAF, and CFP) were required to be gradable. MMI-defined RPD was considered definitely present if (1) there were  $\geq 5$  definite lesions on  $\geq 2$  B-scans on OCT imaging (or OCT-defined RPD), and definite or questionable RPD on at least one *en face* imaging modality, or (2) RPD was definitely present on  $\geq 2$  *en face* imaging modalities.

For all eyes deemed to have definite OCT- and MMI-defined RPD, their extent within the entire central  $20^\circ \times 20^\circ$  region of the OCT volume scan was quantified by another senior grader using NIR and OCT imaging simultaneously. This was performed by manually outlining areas with groups of hyporeflective lesions, with or without a central hyper- or isoreflective core, on NIR imaging that spatially corresponded to definite RPD on OCT B-scans (Fig.). The *en face* area of RPD present in the entire scan area, as well as within each sector sampled on microperimetry (defined above) and outside the central 3.6-mm diameter region, was derived and square root transformed to also eliminate heteroskedasticity of the untransformed measurements.

### Statistical Analysis

Multivariable linear mixed-effect models were used to first examine the associations between overall mean visual sensitivity with RPD presence and extent in the entire OCT volume scan region (described as being at the “eye level”) separately, accounting for correlations between two eyes of the same individual. Each model was adjusted for the potential confounders of age,<sup>43</sup> drusen volume in the central 3.6-mm region,<sup>34,35</sup> and presence of pigmentary abnormalities,<sup>34</sup> in order to examine the independent impact of RPD.

Multivariable linear mixed models were also used to then examine the association between mean sensitivity at each of the five sectors (or “sector-based sensitivity”) with the presence and extent of RPD at each corresponding sector, in order to account for the correlations between the sectors in each eye and between eyes of the same individual. Each model was also adjusted for age, drusen volume in the corresponding sector, and presence of pigmentary abnormalities.

To understand whether sector-based sensitivities were independently associated with both (1) the presence and extent of RPD at the corresponding sector and (2) their presence and extent at the eye level overall, both parameters were included together in similar multivariable linear

**TABLE.** Association Between the Presence or Extent of RPD With Overall Mean Visual Sensitivity or Sector-Based Visual Sensitivity Within the Central 3.6-mm Diameter Region

	RPD Presence (Yes)		RPD Extent (Per mm <sup>*</sup> )	
	Coefficient (95% CI)	P Value	Coefficient (95% CI)	P Value
<b>Overall mean sensitivity (dB)</b>				
Model 1 <sup>†</sup>				
RPD in entire OCT scan	−0.8 (−1.2 to −0.4)	<0.001	−0.3 (−0.4 to −0.2)	<0.001
<b>Sector-based sensitivity (dB)</b>				
Model 2 <sup>‡</sup>				
RPD in each sector	−0.2 (−0.5 to 0.0)	0.073	−0.4 (−0.6 to −0.2)	<0.001
Model 3 <sup>‡</sup>				
RPD in each sector	0.0 (−0.3 to 0.3)	0.804	−0.2 (−0.4 to 0.1)	0.178
RPD in the entire OCT scan	−0.9 (−1.4 to −0.4)	<0.001	−0.3 (−0.4 to −0.1)	<0.001

CI, confidence interval; dB, decibel; OCT, optical coherence tomography volume scan of the central 20° × 20° region.

<sup>\*</sup>Square root transformed.

<sup>†</sup>Adjusted for the presence of pigmentary abnormalities, cube-root drusen volume in the central 3.6-mm diameter region, and age.

<sup>‡</sup>Adjusted for the presence of pigmentary abnormalities, cube-root drusen volume in each corresponding sector, and age.

mixed models described above, adjusting for the same confounders. Statistical analyses were performed using STATA, software version 16.1 (StataCorp, College Station, TX, USA).

## RESULTS

This study included 570 eyes from 285 participants, of whom 209 were female (73%) and the mean age was 70 ± 8 years (range, 51–89 years). A total of 133 (23%) eyes from 73 (26%) participants had definite MMI-defined RPD, which was bilateral in 60 (82%) of the participants. Note that all (100%) eyes with MMI-defined RPD had RPD on OCT. Among the eyes with MMI-defined RPD, the median area with RPD was 13.4 mm<sup>2</sup> (interquartile range, 7.7–22.3 mm<sup>2</sup>), and 132 (99%) of these 133 eyes had RPD present within the central 3.6-mm diameter region sampled on microperimetry testing.

### Association Between RPD and Visual Sensitivity

When evaluating the overall mean sensitivity of all locations in the central 3.6-mm diameter region, both the presence and an increasing extent of RPD at the eye level were independently associated with a significant reduction in visual sensitivity ( $P < 0.001$  for both; [Table](#)).

When evaluating the mean sensitivity of each of the five sectors within the central 3.6-mm region, the presence of RPD in the corresponding sector was not independently associated with a significant reduction in visual sensitivity ( $P = 0.073$ ), but an increasing extent of RPD in the corresponding sector was associated with a reduction in visual sensitivity ( $P < 0.001$ ; [Table](#)).

To examine whether visual sensitivity within each sector was independently associated with both the presence or extent of RPD at each corresponding sector, as well as the overall presence or extent of RPD, both parameters were included together in a multivariable model. The analyses revealed that visual sensitivity at each sector was independently associated with the presence and extent of RPD at the eye level ( $P < 0.001$  for both) but not specifically with their presence and extent in the corresponding sector assessed on microperimetry ( $P = 0.804$  and  $P = 0.178$ , respectively). Note that drusen volume and age were both significant confounders in all the models examined above ( $P < 0.001$  for all), but the presence of pigmentary abnormalities was

not ( $P \geq 0.665$ ). The findings of these confounders for all of these models are presented in their entirety in the Supplementary Materials section.

## DISCUSSION

In this study, we established that the presence and increasing extent of RPD is associated with a significant reduction in mesopic visual sensitivities in the central 3.6-mm region of the macula, reflecting predominantly cone-mediated photoreceptor function,<sup>23–25</sup> even after adjusting for potential confounders of visual sensitivity. However, our analyses uniquely revealed that sector-based visual sensitivities in the central macular region were independently associated with the overall presence and extent of RPD at the eye level, rather than with their presence and extent in the corresponding sector assessed on microperimetry. These findings highlight how an understanding of the impact of RPD on cone photoreceptor function may require consideration of factors beyond the direct impact of RPD on the overlying photoreceptors, warranting further studies to understand pathogenic pathways accounting for these observations.

The findings of this study are consistent with a previous study, which reported that mesopic visual sensitivities were reduced in non-late AMD eyes with coexistent RPD compared to those without RPD.<sup>31</sup> Our findings are also supported by previous studies that have reported a significant correlation between the number of RPD lesions present and visual sensitivity in eyes with only RPD,<sup>44</sup> as well as a significant reduction in visual sensitivity within areas with RPD compared to those without.<sup>18</sup> Overall, this study contributes to the body of evidence available to date implicating cone photoreceptor dysfunction in eyes with RPD.

This study also replicated findings from our previous study, where we did not observe a significant difference in sector-based visual sensitivities within the central 3-mm region based on the presence of RPD in the corresponding sector.<sup>34</sup> While these sector-based visual sensitivities were significantly associated with the quantitative *en face* extent of RPD in each corresponding sector, further analyses revealed that the overall presence and extent of RPD at the eye level was independently associated with these sector-based sensitivities, not the presence or extent of RPD in the corresponding sectors.

Importantly, this study revealed that observable structure-function associations at the regional level (i.e., within sectors) for mesopic visual sensitivities are primarily explained by the overall extent of RPD at the eye level. These findings suggest that the overall extent of RPD in an eye may potentially be an indicator of other generalized pathogenic changes occurring that are associated with the observed visual deficits reflecting predominant cone photoreceptor dysfunction, beyond the direct impact of the RPD lesions on the overlying photoreceptors.<sup>14-17</sup> The notion that eyes with RPD show reduced visual sensitivities beyond where the lesions are present was also suggested in a recent study based on observations that foveal mesopic visual sensitivity was significantly reduced in eyes with predominantly RPD compared to eyes with only drusen (and without RPD) and healthy eyes, despite RPD being absent at the fovea for all the eyes with RPD.<sup>45</sup> While this study included only 30 eyes and did not perform adjustments for key confounders such as drusen volume, their observations lend support to the findings in this study.

These findings warrant further studies to understand the impact of RPD on cone photoreceptor function, which may in turn help uncover new insights into the disease mechanisms behind RPD development. Such studies could evaluate changes in the photoreceptor support systems—the RPE, Bruch's membrane and choriocapillaris—whose changes have been implicated as the pathogenesis of AMD, subsequently leading to photoreceptor dysfunction and death.<sup>46</sup> Such changes on OCT imaging could potentially be identified using artificial intelligence, to enable an agnostic approach to biomarker discovery, an approach used in a recent study seeking to understand the structural basis of rod photoreceptor dysfunction.<sup>47</sup>

Limitations of this study include the evaluation of only a subset of individuals with the earlier stages of AMD, namely, those with bilateral large drusen, and the generalizability to others without large drusen is thus unknown. However, strengths of this study include the large size of the cohort, adjustment for potential confounders of visual sensitivity, and the evaluation of the quantitative *en face* extent of RPD.

In conclusion, we established that the presence and increasing extent of RPD at the eye level was independently associated with a significant reduction in mesopic visual sensitivity in the macular region, underscoring cone photoreceptor dysfunction in association with RPD. However, further evaluation revealed that visual sensitivities at specific sectors in this central region were explained by the overall presence or extent of RPD, rather than their presence or extent of RPD in the topographically corresponding sector assessed on microperimetry. These findings suggest that there may be generalized pathogenic changes occurring in eyes with RPD that account for the observed visual sensitivity deficits reflective primarily of cone-mediated photoreceptor dysfunction, encouraging further exploration that could uncover new insights into the impact and the implications of this phenotype in AMD.

### Acknowledgments

Supported by the National Health & Medical Research Council of Australia (grants APP1181010 [RHG, ZW] and fellowship GNT1103013 [RHG]) and a Macular Disease Foundation Australia grant (ZW, RHG). The Centre for Eye Research Australia receives operational infrastructure support from the Victorian Government. The funders had no role in the

manuscript writing and the decision to submit the manuscript for publication.

Disclosure: **H. Kumar**, None; **R.H. Guymer**, Bayer (F), Novartis (F), Roche Genentech (F), Apellis (F); **L.A.B. Hodgson**, None; **X. Hadoux**, None; **Z. Wu**, None

### References

1. Wu Z, Ayton LN, Luu CD, Baird PN, Guymer RH. Reticular pseudodrusen in intermediate age-related macular degeneration: prevalence, detection, clinical, environmental and genetic associations. *Invest Ophthalmol Vis Sci*. 2016;57:1310–1316.
2. Gabrielle P-H, Seydou A, Arnould L, et al. Subretinal drusenoid deposits in the elderly in a population-based study (the Montrachet Study). *Invest Ophthalmol Vis Sci*. 2019;60:4838–4848.
3. Wu Z, Fletcher EL, Kumar H, Greferath U, Guymer RH. Reticular pseudodrusen: a critical phenotype in age-related macular degeneration. *Prog Retin Eye Res*. 2021;88:101017.
4. Zhou Q, Shaffer J, Ying G-s. Pseudodrusen in the fellow eye of patients with unilateral neovascular age-related macular degeneration: a meta-analysis. *PLoS One*. 2016;11:e0149030.
5. Finger RP, Wu Z, Luu CD, et al. Reticular pseudodrusen: a risk factor for geographic atrophy in fellow eyes of individuals with unilateral choroidal neovascularization. *Ophthalmology*. 2014;121:1252–1256.
6. Zhou Q, Daniel E, Maguire MG, et al. Pseudodrusen and incidence of late age-related macular degeneration in fellow eyes in the Comparison of Age-Related Macular Degeneration Treatments Trials. *Ophthalmology*. 2016;123:1530–1540.
7. Nassisi M, Lei J, Abdelfattah NS, et al. OCT risk factors for development of late age-related macular degeneration in the fellow eyes of patients enrolled in the HARBOR Study. *Ophthalmology*. 2019;126:1667–1674.
8. Luu CD, Tan R, Caruso E, et al. Topographic rod recovery profiles after a prolonged dark adaptation in subjects with reticular pseudodrusen. *Ophthalmol Retina*. 2018;2:1206–1217.
9. Tan RS, Guymer RH, Aung KZ, Caruso E, Luu CD. Longitudinal assessment of rod function in intermediate age-related macular degeneration with and without reticular pseudodrusen. *Invest Ophthalmol Vis Sci*. 2019;60:1511–1518.
10. Flamendorf J, Agron E, Wong WT, et al. Impairments in dark adaptation are associated with age-related macular degeneration severity and reticular pseudodrusen. *Ophthalmology*. 2015;122:2053–2062.
11. Flynn OJ, Cukras CA, Jeffrey BG. Characterization of rod function phenotypes across a range of age-related macular degeneration severities and subretinal drusenoid deposits. *Invest Ophthalmol Vis Sci*. 2018;59(6):2411–2421.
12. Guymer RH, Wu Z, Hodgson LAB, Caruso E, Brassington KH, Tindill N, et al. Subthreshold nanosecond laser intervention in age-related macular degeneration: the LEAD randomized controlled clinical trial. *Ophthalmology*. 2019;126(6):829–838.
13. Greferath U, Guymer RH, Vessey KA, Brassington K, Fletcher EL. Correlation of histologic features with in vivo imaging of reticular pseudodrusen. *Ophthalmology*. 2016;123(6):1320–1331.
14. Zweifel SA, Spaide RF, Curcio CA, Malek G, Imamura Y. Reticular pseudodrusen are subretinal drusenoid deposits. *Ophthalmology*. 2010;117(2):303–312.e1.
15. Querques G, Canoui-Poitrine F, Coscas F, et al. Analysis of progression of reticular pseudodrusen by spectral domain-optical coherence tomography. *Invest Ophthalmol Vis Sci*. 2012;53:1264–1270.

16. Mrejen S, Sato T, Curcio CA, Spaide RF. Assessing the cone photoreceptor mosaic in eyes with pseudodrusen and soft drusen in vivo using adaptive optics imaging. *Ophthalmology*. 2014;121:545–551.
17. Zhang Y, Wang X, Rivero EB, et al. Photoreceptor perturbation around subretinal drusenoid deposits revealed by adaptive optics scanning laser ophthalmoscopy. *Am J Ophthalmol*. 2014;158:584–596.e1.
18. Sasmannshausen M, Pfau M, Thiele S, et al. Longitudinal analysis of structural and functional changes in presence of reticular pseudodrusen associated with age-related macular degeneration. *Invest Ophthalmol Vis Sci*. 2020;61(10):19.
19. Chiang TT-K, Keenan TD, Agrón E, et al. Macular thickness in intermediate age-related macular degeneration is influenced by disease severity and subretinal drusenoid deposit presence. *Invest Ophthalmol Vis Sci*. 2020;61(6):59.
20. Ramon C, Cardona G, Biarnés M, Ferraro LL, Monés J. Longitudinal changes in outer nuclear layer thickness in soft drusen and reticular pseudodrusen. *Clin Expl Optom*. 2019;102:601–610.
21. Nittala MG, Hogg RE, Luo Y, et al. Changes in retinal layer thickness in the contralateral eye of patients with unilateral neovascular age-related macular degeneration. *Ophthalmol Retina*. 2019;3:112–121.
22. Pfau M, Jolly JK, Wu Z, et al. Fundus-controlled perimetry (microperimetry): application as outcome measure in clinical trials. *Prog Retin Eye Res*. 2021;82:100907.
23. Crossland MD, Tufail A, Rubin GS, et al. Mesopic microperimetry measures mainly cones; dark-adapted microperimetry measures rods and cones. *Invest Ophthalmol Vis Sci*. 2012;53(14):4822.
24. Simunovic MP, Moore AT, MacLaren RE. Selective automated perimetry under photopic, mesopic, and scotopic conditions: detection mechanisms and testing strategies. *Transl Vis Sci Technol*. 2016;5(3):10.
25. Han RC, Gray JM, Han J, et al. Optimisation of dark adaptation time required for mesopic microperimetry. *Br J Ophthalmol*. 2019;103(8):1092–1098.
26. Ooto S, Ellabban AA, Ueda-Arakawa N, et al. Reduction of retinal sensitivity in eyes with reticular pseudodrusen. *Am J Ophthalmol*. 2013;156:1184–1191.e2.
27. Querques G, Massamba N, Srour M, et al. Impact of reticular pseudodrusen on retinal function. *Retina*. 2014;34:321–329.
28. Corvi F, Souied EH, Falfoul Y, et al. Pilot evaluation of short-term changes in macular pigment and retinal sensitivity in different phenotypes of early age-related macular degeneration after carotenoid supplementation. *Br J Ophthalmol*. 2017;101:770–773.
29. Corvi F, Pellegrini M, Belotti M, Bianchi C, Staurengi G. Scotopic and fast mesopic microperimetry in eyes with drusen and reticular pseudodrusen. *Retina*. 2019;39:2378–2383.
30. Forte R, Cennamo G, De Crecchio G, Cennamo G. Microperimetry of subretinal drusenoid deposits. *Ophthalmic Res*. 2014;51:32–36.
31. Ooto S, Suzuki M, Vongkulsiri S, Sato T, Spaide RF. Multimodal visual function testing in eyes with nonexudative age-related macular degeneration. *Retina*. 2015;35:1292–1302.
32. Steinberg JS, Saßmannshausen M, Fleckenstein M, et al. Correlation of partial outer retinal thickness with scotopic and mesopic fundus-controlled perimetry in patients with reticular drusen. *Am J Ophthalmol*. 2016;168:52–61.
33. Wu Z, Cunefare D, Chiu E, et al. Longitudinal associations between microstructural changes and microperimetry in the early stages of age-related macular degeneration. *Invest Ophthalmol Vis Sci*. 2016;57:3714–3722.
34. Wu Z, Ayton LN, Makeyeva G, Guymer RH, Luu CD. Impact of reticular pseudodrusen on microperimetry and multifocal electroretinography in intermediate age-related macular degeneration. *Invest Ophthalmol Vis Sci*. 2015;56:2100–2106.
35. Ponderfer SG, Wintergerst MWM, Gorgi Zadeh S, et al. Association of visual function measures with drusen volume in early stages of age-related macular degeneration. *Invest Ophthalmol Vis Sci*. 2020;61(3):55.
36. Lek JJ, Brassington KH, Luu CD, et al. Subthreshold nanosecond laser intervention in intermediate age-related macular degeneration: study design and baseline characteristics of the Laser in Early Stages of Age-Related Macular Degeneration Study (report number 1). *Ophthalmol Retina*. 2017;1:227–239.
37. Ferris FL, Wilkinson CP, Bird A, et al. Clinical classification of age-related macular degeneration. *Ophthalmology*. 2013;120:844–851.
38. Wu Z, Luu CD, Ayton LN, et al. Optical coherence tomography defined changes preceding the development of drusen-associated atrophy in age-related macular degeneration. *Ophthalmology*. 2014;121:2415–2422.
39. Wu Z, Luu CD, Hodgson LA, et al. Prospective longitudinal evaluation of nascent geographic atrophy in age-related macular degeneration. *Ophthalmol Retina*. 2020;4:568–575.
40. Stockman A, Sharpe LT. Into the twilight zone: the complexities of mesopic vision and luminous efficiency. *Ophthalmic Physiol Opt*. 2006;26(3):225–239.
41. Wu Z, Ayton LN, Guymer RH, Luu CD. Intrasession test-retest variability of microperimetry in age-related macular degeneration. *Invest Ophthalmol Vis Sci*. 2013;54:7378–7385.
42. Gorgi Zadeh S, Wintergerst MWM, Wiens V, et al. CNNs enable accurate and fast segmentation of drusen in optical coherence tomography. In: Cardoso MJ, Arbel T, Carneiro G, et al., eds. *Deep Learning in Medical Image Analysis and Multimodal Learning for Clinical Decision Support*. Cham, Switzerland: Springer International Publishing; 2017.
43. Roh M, Láins I, Shin HJ, et al. Microperimetry in age-related macular degeneration: association with macular morphology assessed by optical coherence tomography. *Br J Ophthalmol*. 2019;103:1769.
44. Ooto S, Ellabban AA, Ueda-Arakawa N, et al. Reduction of retinal sensitivity in eyes with reticular pseudodrusen. *Am J Ophthalmol*. 2013;156:1184–1191.e2.
45. Zhang Y, Sadda SR, Sarraf D, et al. Spatial dissociation of subretinal drusenoid deposits and impaired scotopic and mesopic sensitivity in AMD. *Invest Ophthalmol Vis Sci*. 2022;63(2):32.
46. Bhutto I, Lutty G. Understanding age-related macular degeneration (AMD): relationships between the photoreceptor/retinal pigment epithelium/Bruch's membrane/choriocapillary complex. *Mol Aspects Med*. 2012;33(4):295–317.
47. Lee AY, Lee CS, Blazes MS, et al. Exploring a structural basis for delayed rod-mediated dark adaptation in age-related macular degeneration via deep learning. *Transl Vis Sci Technol*. 2020;9(2):62.